Journal of Chromatography, 316 (1984) 211–225
Elsevier Science Publishers B.V., Amsterdam — Printed in The Netherlands

CHROMSYMP. 459

UV VISUALIZATION OF INORGANIC ANIONS BY REVERSED-PHASE ION-INTERACTION CHROMATOGRAPHY: FACTORS THAT CONTROL SENSITIVITY AND DETECTION

WILLIAM E. BARBER
Hercules Research Center, Wilmington, DE 19894 (U.S.A.)
and
PETER W. CARR*
Chemistry Department, University of Minnesota, Minneapolis, MN 55455 (U.S.A.)

SUMMARY

This paper describes a chromatographic technique and detection scheme for inorganic anion analysis. Factors that affect sensitivity and detection are discussed, including the concentration and molar absorptivity of the ion-interaction reagent (IIR) as well as the retention of the eluite ion relative to the retention of the system peak.

An ideal system will employ a low IIR concentration, so that a detection wavelength corresponding to a high IIR molar absorptivity can be used to monitor the eluites. In addition, eluites that are eluted before the system peak have much lower response factors than those eluted after the system peak. Furthermore, eluites that are not well separated from the system peak have response factors that are many times larger than eluites that are eluted either before or after the system peak. Computer simulations were performed that predict these response factors.

INTRODUCTION

In the past few years there have been several reports dealing with the chromatographic separation of inorganic anions on bonded-phase columns and UV detection[1–6]. One approach has been to monitor elution of UV-absorbing anions directly at low wavelengths (205–220 nm)[1–4]. An ion chromatographic column has also been used with direct UV monitoring of anions[5]. Small and Miller[6] have introduced an indirect photometric technique for detecting anions that utilizes an ion-chromatographic column with a UV-absorbing eluent. Vacancy peaks are induced for each sample ion that displaces the UV-absorbing buffer ions from the ion-exchange surface of the column packing.

A number of workers have reported another indirect photometric detection technique that utilizes bonded-phase columns[7–19]. Early work in this area dealt with the analysis of organic ions such as bile acids[7], carboxylic and amino acids[8], alkyl sulfonates[9,10] and alkyl amines[10]. Bidlingmeyer and Warren[17,18] and Hackzell *et*

0021-9673/84/$03.00

al.[10] have reported the effect of sample and eluent composition on quantitation in systems for the determination of organic ions.

More recently, this UV-visualization detection technique has been applied to the analysis of inorganic anions with bonded-phase columns in an ion-interaction mode[13–16,19]. Previous reports from this laboratory[13–16] have dealt with the design of the chromatographic systems necessary to effect suitable separations on a bonded-phase column and with the factors that control retention and selectivity of inorganic ions in these systems.

The present report deals with the factors that affect sensitivity and detection. These include the concentration and absorptivity of the ion-interaction reagent (IIR), the retention of the sample peaks relative to the retention of the IIR (system peak), as well as detector noise characteristics.

Previous reports[8,10] have advocated the adjustment of chromatographic conditions so that samples are eluted near the system peak to take advantage of the enhanced sensitivity which occurs under these conditions. In this report, we propose that samples should be made to emerge after the system peak in the region where sensitivity is nearly constant for all UV-transparent ions.

In addition, we have performed chromatographic simulations that include the presence of buffer ions, in addition to the IIR, in the eluent. These simulations predict the existence of two system peaks. One of these system peaks emerges at the column void volume and the other at a volume characteristic of the IIR. Further, the model successfully predicts qualitatively the observed variations in sensitivity for samples which are less retained, equally retained, and more retained than the IIR system peak.

These simulations also show that the true mechanism (kinetics) of retention is irrelevant to the detection scheme, provided that the thermodynamic model allows the stationary phase concentration of the IIR to be locally perturbed by the presence of a sample ion.

EXPERIMENTAL

The chromatographic technique (*i.e.* hardware, reagents, and preparation of eluents) has been described in detail in earlier reports[13–16].

The computer system used for the simulations consisted of an Apple II Plus computer, dual floppy disk drives, and an Epson MX-80 dot matrix printer. The software that performed the chromatographic simulations was written in BASIC but executed in compiled BASIC. The algorithm is based on a Craig-type repetitive distribution model[20] with multiple simultaneous equilibria. The source code for this software can be found elsewhere[15].

RESULTS AND DISCUSSION

An in-depth, theoretical description of the indicator mechanism for visualization of UV-transparent samples, based on UV-absorbing ion-interaction reagents (IIRs) has been presented by Stranahan and Deming[21]. The detector monitors a constant background absorbance due to the IIR in the eluent. A change in the signal is produced at the detector when a sample, upon injection into the column perturbs

the distribution equilibrium of the IIR. This causes a certain amount of IIR to be either adsorbed from the eluent onto the stationary phase or desorbed from the stationary phase into the eluent. This perturbation will advance along the column at the same rate as the sample or the IIR. When the eluite or system zone emerges from the column, the perturbation of the eluent concentration of IIR will also emerge thereby changing the absorbance reading of the detector (either a positive or negative peak will appear). Ignoring for the moment the increase in background noise attributed to increasing the background absorbance of a detector (see below), the sensitivity of the method should improve in proportion to an increase in the extinction coefficient of the IIR. This would be due to the larger net change in absorbance at the detector for a given perturbation in the eluent IIR concentration. It should be emphasized that this change in sensitivity should be directly related to the change in the extinction coefficient of the IIR and will manifest itself as a change in the slope of a calibration curve of peak height or area versus concentration of sample injected.

Table I is a summary of sensitivities and detection limits of various anions determined under different experimental conditions. The extinction coefficient was varied by changing the wavelength of detection. In addition, the background absorbance was varied in two ways. First, the wavelength was held constant and the concentration of IIR was varied. Secondly, the IIR concentration was held constant and the wavelength of detection was varied. It is evident from these data that the sensitivity or slope of the calibration curve does indeed increase upon increasing the extinction coefficient of the IIR. The ratio of extinction coefficients for eluents C over A (4.48) predicts a similar ratio of the sensitivities (slopes) and detection limits for the two calibration curves. The actual ratios turn out to be about 20% and 16% lower for the slopes (3.58) and detection limits (3.75), respectively. Considering that another variable, specifically the concentration and nature of the alkyl sulfonate, was also changed, the agreement between these figures is reasonable. The necessity of adding an alkyl sulfonate to the eluent in order to reduce the k' of the system peak

TABLE I

SENSITIVITY AND DETECTION LIMIT AS A FUNCTION OF IIR ABSORPTIVITY FOR PEAK AREA *VS.* NANOMOLES INJECTED

Slope = AU-sec/nanomoles; % σ = (σ/slope) × 100; [IIR] = concentration of naphthylmethyltributylammonium hydroxide in m*M*; n = number of points; D.L. = detection limit in nanomoles injected. Eluents: A = 4 m*M* α-IIR, 0.25 m*M* hexanesulfonate, 10 m*M* pH 4.75 acetic acid–acetate buffer; B = 4 m*M* β-IIR, 0.2 m*M* heptanesulfonate, 10 m*M* pH 4.75 acetic acid–acetate buffer; C = 1 m*M* β-IIR, 0.5 m*M* octanesulfonate, 10 m*M* pH 4.75 acetic acid–acetate buffer.

Anion	*[IIR]*	*Eluent*	*λ (nm)*	*ε*	*n*	*Slope ± % σ*	*D.L.*
Chloride	4	A	316	424	23	0.00642 ± 0.83	0.6
Nitrite	4	A	316	424	21	0.00634 ± 1.03	0.7
Bromide	4	A	316	424	22	0.00754 ± 0.52	0.3
Nitrate	4	A	316	424	20	0.00806 ± 1.22	0.8
Sulfate	4	B	309	500	25	0.01104 ± 0.30	0.3
Thiosulfate	4	B	309	500	25	0.01136 ± 0.66	0.6
Pentanesulfonate	1	C	293	1900	17	0.0278 ± 0.34	0.08
Iodide	1	C	293	1900	18	0.0245 ± 1.66	0.7
Hexanesulfonate	1	C	293	1900	26	0.0239 ± 2.72	0.2

to a value less than 2 was discussed in earlier reports[13–16]. The ratio for the slopes was calculated from the average slopes for each eluent. The ratio for the detection limits was calculated from the values for bromide and pentanesulfonate, which have the most similar precisions in A and C. This is necessary for a valid comparison, because the detection limits, as calculated, are a function of measurement precision when the method of Hubaux and Vos[22] is used.

It is evident from the above discussion that the sensitivity can be improved by increasing the extinction coefficient of the IIR. However there is a limit to how large the extinction coefficient can be made. The product of the extinction coefficient and the IIR concentration determines the background absorbance of the eluent at a particular wavelength of detection. As the background absorbance of the eluent increases, the peak-to-peak detector noise also increases. Above about 1.0 AU background absorbance, for a Perkin-Elmer LC-55 detector, the detector noise increases rapidly, and the signal-to-noise ratio begins to decrease, as described below.

Fig. 1A is a plot of peak-to-peak noise *versus* background absorbance. These data were obtained by pumping 0, 1, 2 and 3 m*M* *p*-nitrobenzyltributylammonium hydroxide, dissolved in aqueous 10 m*M* acetic acid–sodium acetate buffer, through the chromatograph column at a flow-rate of 2.0 ml/min. When the system was at equilibrium, the background absorbance, if any, was balanced out by using a DC-offset[15], so that the noise fluctuation could be recorded on a strip-chart recorder with an expanded scale. The peak-to-peak AU value was then measured with a ruler. The noise increases about linearly with the background absorbance up to an absorbance of 1.0 AU for the Perkin-Elmer LC-55 detector used in this study. At absorbances higher than 1.0 AU the increase in noise becomes quite nonlinear and very rapidly increases, as shown in Fig. 1. At absorbances less than 1.0 AU the increase in sensitivity due to higher extinction coefficients is proportionately larger than the increase in noise for a net increase in the signal-to-noise ratio. For example, Fig. 1B shows what happens to the signal-to-noise ratio as the concentration of the IIR in the eluent is increased. These data were derived from Fig. 1A and are the signal-to-noise ratio for the IIR in the eluent. A small perturbation in the background absorbance due to the injection of a sample should have approximately the same signal-to-noise ratio. The data in Fig. 1B show that the signal-to-noise ratio increases up to a background absorbance of approximately 1.0 AU, but then the noise characteristics of the detector take over and the signal-to-noise ratio starts to decrease. Therefore, no increase in detectability is gained by working at background absorbances higher than 1.0 AU.

Fig. 1B contains the same data as Fig. 1A, but they are plotted in a manner that is more familiar to discussions of noise limitations versus percent transmittance in photometric detectors[23]. This is a plot of the relative uncertainty as a function of background absorbance and shows a minimum at about 1 AU. A comprehensive discussion of different types of noise limitations of photometric systems as a function of absorbance can be found elsewhere[23]. The noise characteristics of the detector used in this study seem to be a function of two types of noise limitations. The minimum in the curve (approx. 1 AU) coincides with that normally found for photometers that are precision-limited by photocurrent shot noise, particularly at low absorbance values. However, the plot curves up rapidly above 1 AU, which is more characteristic of a photometer limited by dark-current shot noise. This is quite reasonable, since it is very uncommon to find a conventional spectrophotometer limited only by pho-

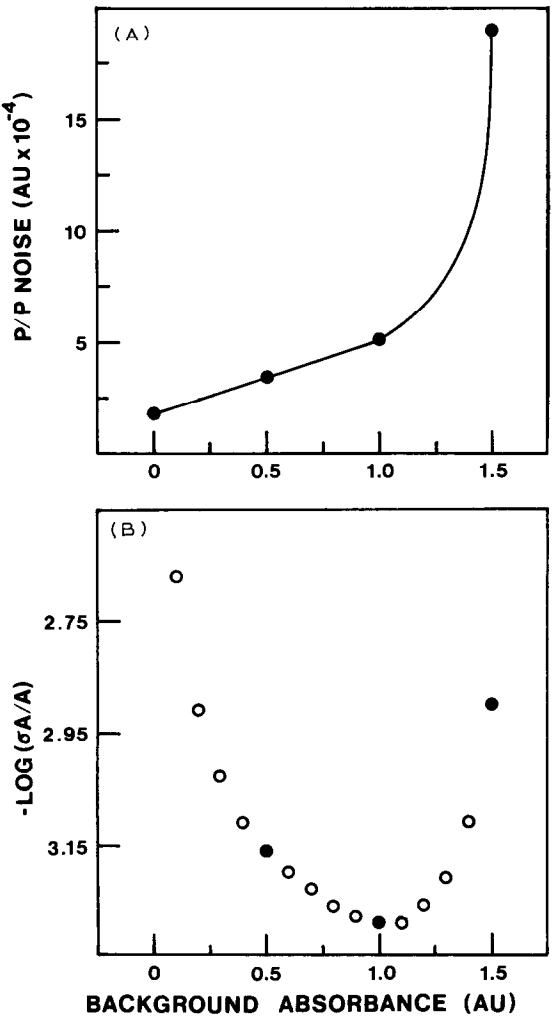

Fig. 1. Detector noise *versus* background absorbance. Conditions: Perkin-Elmer LC-55 variable-wavelength detector. Other conditions as described in the text. (A) Experimental values of peak-to-peak noise *versus* background absorbance. (B) Closed symbols are actual experimental points. Open symbols are interpolated points, derived from A.

tocurrent shot noise[23]. Dark-current shot noise is usually dominant when the light source intensity is low in a particular wavelength region, which suggests that for our work a detector with a source of higher intensity would allow us to work at even higher background absorbances without compromising sensitivity with a drastic increase in noise. In any case, the results found for the photometric detector used in this work are qualitatively similar to those expected for conventional spectrophotometers.

A balance is needed between the concentration of IIR, and the wavelength of detection, which then determines the extinction coefficient, in order to develop a

working system. The best way to proceed is to determine the lowest concentration of IIR that will effect a suitable separation. This will entail not only changing the concentration of the IIR but also the concentration of the alkyl sulfonate that is added to reduce the k' of the system peak. This problem has been discussed in earlier reports[13–16]. Once the optimum concentration of IIR has been determined, the wavelength of detection is changed until the background absorbance reading is about 1.0 AU. This effectively maximizes the extinction coefficient and affords the best sensitivity and detection limits obtainable with the given eluent IIR concentration.

It should be evident that it is best to work with very low concentrations of IIR and take advantage of the high sensitivities obtainable with the resultant high extinction coefficients. This is not always possible for reasons discussed in earlier reports[13–16].

The sensitivity or response for a sample peak depends very strongly on the sample capacity factor (k') relative to the system peak. Our observation[13–16] that there is an enhanced sensitivity when sample and system peaks nearly coincide, is in general agreement with those of others[8–11,17–18,21]. Specifically, the response for a peak with a k' less than the system peak is very low. As the k' for the sample approaches that for the system peak, there is generally an enhanced sensitivity for both the sample and the system peak. This enhanced response amounts to many times the response obtained when an equimolar amount of IIR alone is injected. As the k' of the sample becomes larger than that of the system peak, the response once again decreases, but at high k' values (relative to the system peak) the response levels out and becomes nearly constant. A number of other workers have also observed similar effects[8,10,17,18].

Fig. 2 is a series of three chromatograms where the experimental conditions are identical, except that the buffer concentration is decreased from 25 to 10 to 5 mM, which results in an increase in sample retention and a slight increase in the system peak k'. The generally low and then rapid rise in response is particularly evident for chloride as its k' is increased from a low value relative to the system peak to values approaching that of the system peak. The enhanced response for a peak that emerges quite near the system peak is observed for bromide and nitrite in chromatograms A and B, respectively. The leveling out of the response in terms of the area for each peak is observed for the bromide and nitrate peaks in chromatogram B, where their areas are seen to be about equal. This effect is also seen in chromatogram C for nitrite, bromide, and nitrate.

It is very tempting to take advantage of the enhanced response that can be obtained by optimizing the eluent conditions so that the majority of sample species emerge near the system peak. Some workers have advocated this approach[8,10].

It has been our experience that quantitative precision is very poor for an eluite that emerges near the system peak and therefore gives this enhanced response. This is due to the fact that the UV-visualization technique is based on a dynamic equilibrium, *i.e.* very slight changes in experimental parameters, such as temperature or ionic strength, will shift the k' of the sample ions slightly. This normally causes no problems in conventional HPLC detection (UV or RI), since area is conserved. In UV-visualization detection the response for a sample species is very dependent on k' as shown in Fig. 3. When the eluite and system peak have similar k' values, a slight change in eluite k' results in a dramatic change in response.

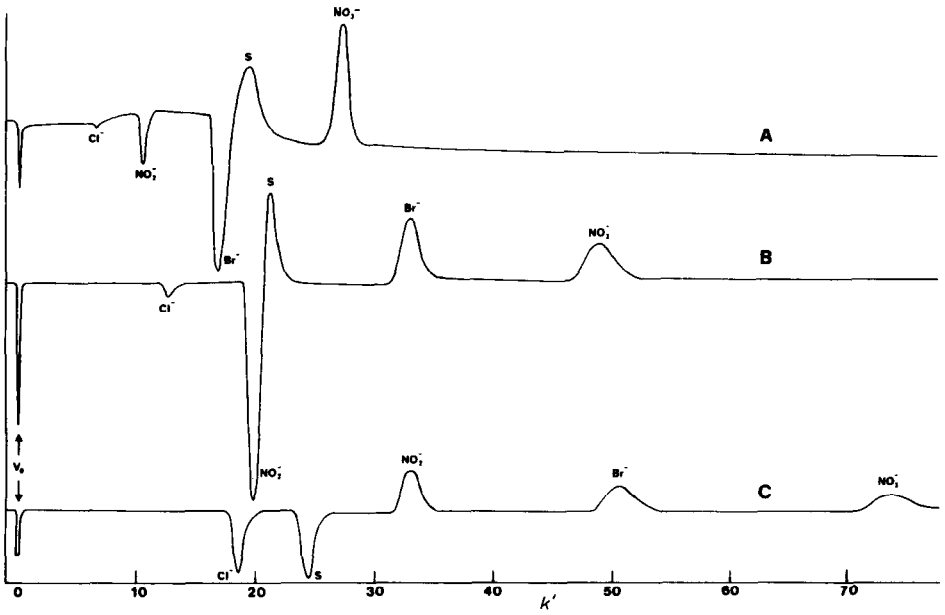

Fig. 2. Experimental chromatograms, showing the effect of sample peak k' relative to the system peak on the peak response. Chromatographic conditions: 0.5 mM Naphthylmethyltributylammonium chloride, acetic acid–acetate buffer, pH 4.75. (A) 25 mM buffer; (B) 10 mM buffer; (C) 5 mM buffer.

Instead of optimizing a separation so that samples and the system peak have similar retention, one could obtain an ideal separation when all eluite ions emerge after the system peak, which should have a very low retention. This would mean sacrificing the enhanced sensitivity that results when eluite and system peaks emerge almost simultaneously, but another advantage would be gained. This advantage is the nearly constant and increased response that is predicted for all eluites that emerge after the system peak (in contrast to those that emerge prior to the system peak), as shown in Fig. 4. This prediction is experimentally verified for inorganic anions that are eluted after the system peak. The ions listed in Table II all have retentions that are larger than the system peak. This table contains the sensitivities for each ion, corrected for the extinction coefficient of the IIR in terms of peak area. It is evident from these data that sensitivity varies either very little with relative k' or as a function of the chromatographic conditions, which are quite different for eluents A and C. The largest ratio is only about 1.8. Based on these data, we may conclude that detection by this technique of UV visualization is nearly nonspecific when the eluite ions emerge after the system peak unless the eluite ion itself absorbs strongly at the detection wavelength.

When the sensitivities, as defined in Table II, are normalized to the sensitivity for the IIR (injected as a sample) the normalized response factors in Table III are obtained for four representative anions. The average of these response factors is essentially 1.0, indicating that an equivalent amount of IIR migrates through the column in the local region of the sample zone. The slight increase in response factors

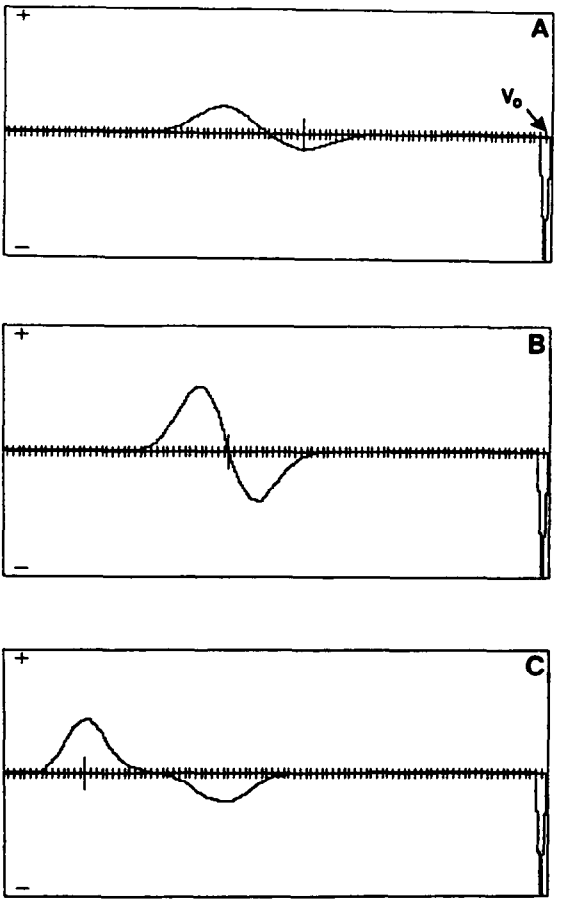

Fig. 3. Representative simulation plots for a ion-pair mechanism with buffer ions. Number of tubes(transfers) = 99; [IIR] = 10 *M*; [buffer] = 20 *M*; [sample] = 2 *M*; K_A = 1 ml/mole; K_B = 0.5 ml/mole; K_{BX} = 100 ml/g; phase ratio = 1 g/ml. (A) K_{AX} = 85 ml/g, k' (IIR) = 1.54, k' (sample) = 0.83; (B) K_{AX} = 140 ml/g, k' (IIR) = 1.51, k' (sample) = 1.41; (C) K_{AX} = 550 ml/g, k' (IIR) = 1.48, k' (sample) = 5.60. Vertical slash indicates the position of the maximum sample concentration.

for sample ions with increasing k' values has also been observed by others[8] for organic ions.

The sensitivity effects described above can be theoretically predicted. Stranahan and Deming[21] have reported simulations that predict the induction of both deficient and excess concentration zones of a mobile-phase component when the distribution equilibrium of that mobile phase component is perturbed upon injection of a sample. The two simulations that they performed are both based on a Craig-type repetitive distribution model[20]. The mechanism for their first simulation is completely general. The only other assumption made, beyond the assumption that the distribution of the sample is affected by the mobile and stationary phase compositions, is that the distributions of the mobile phase components are perturbed by the local presence of the sample[24,25].

TABLE II

NORMALIZED SENSITIVITY *VS.* RETENTION FOR IONS MORE RETAINED THAN THE SYSTEM PEAK

[IIR] = Concentration of naphthylmethyltributylammonium hydroxide in m*M*. Sens = Slope from Table I divided by ε and then multipled by 100,000. Eluents A–C as in Table I.

Anion	*[IIR]*	*Eluent*	λ	ε	*k'*	*Sens*
Chloride	4	A	316	424	3.48	1.51
Nitrite	4	A	316	424	5.02	1.50
Bromide	4	A	316	424	7.84	1.78
Nitrate	4	A	316	424	11.5	1.90
Sulfate	4	B	309	500	6.61	2.21
Thiosulfate	4	B	309	500	9.87	2.27
Pentanesulfonate	1	C	293	1900	4.63	1.46
Iodide	1	C	293	1900	6.41	1.29
Hexanesulfonate	1	C	293	1900	15.6	1.26

For a sample that causes increased adsorption of IIR in the vicinity of the sample ion the sample peak will be negative and the system peak positive if the eluite emerges before the system peak. For a sample that emerges after the system peak the opposite is true. The enhanced sensitivity that is experimentally observed when eluite and system peak emerge together is also predicted by their model[21].

The simulation described above was for the completely general model, where no specific mechanism of adsorption–desorption is implied. Stranahan and Deming are among the proponents of the ion-interaction mechanism of ionized solute retention in the presence of an oppositely charged mobile phase IIR[24–26]. The second series

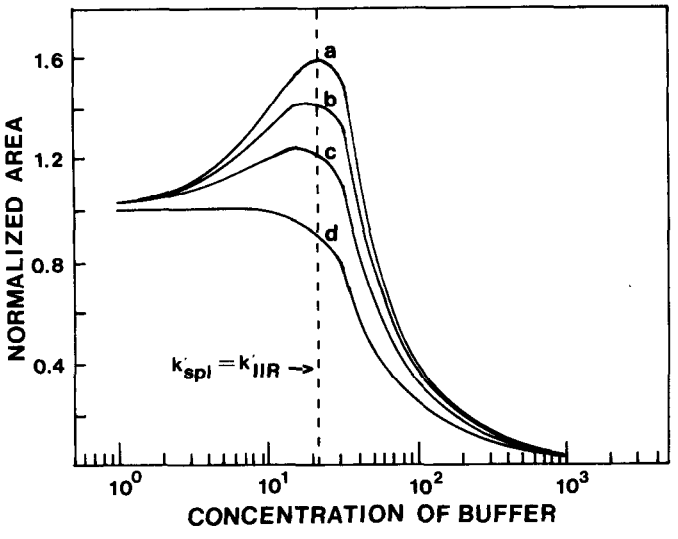

Fig. 4. Response factor curves as a function of (1) the concentration of buffer (which varies the relative *k'* of system and sample peaks) and (2) the number of tubes (transfers). a = 99; b = 75; c = 50; d = 25 transfers.

TABLE III

NORMALIZED RESPONSE FACTORS FOR FOUR REPRESENTATIVE ANIONS

Chromatographic conditions: 4 m*M* naphthylmethyltributylammonium hydroxide, 0.25 m*M* hexanesulfonate, 10 m*M*, pH 4.75 acetic acid–acetate buffer. Sens = 100,000 × [AU-sec/(mole × ε)]. Response factor = Sens (sample)/Sens (system). Detection wavelength = 316 nm.

Anion	*k'*	Sens	Response factor
Chloride	3.48	1.55	0.90
Nitrite	5.02	1.54	0.90
Bromide	7.84	1.79	1.04
Nitrate	11.5	1.94	1.13
			0.99 = average
System	2.36	1.72	

of simulations they performed were based on this model of retention when the general equations of adsorption used in the equilibrium stages of the first simulation are replaced by those derived for an ion-interaction mechanism of retention[21,26]. The results of this second simulation showed, that if retention followed an ion-interaction mechanism, the same general phenomena would occur as predicted in the first case where no mechanism was specified. Positive or negative peaks were observed for the eluite, depending on the order of elution of sample and IIR zones. The specific calculations involved in this mechanism for retention can be found in their papers[21,26].

Stranahan and Deming did not report the relative sensitivities for peaks that emerged before and after the system peak in their simulations. From the figures published in their report[21] it appeared that an eluite peak gives an identical absolute response (area) whether it is eluted before or after the system peak. Our experimental work with inorganic anions (see Fig. 2) shows clearly that eluites that emerge before the system peak have a much lower sensitivity (area) than those that emerge after the system peak.

The purpose of the following discussion is to present the results of a simulation based on the arbitrary assumption of ion-pair formation in the mobile phase and subsequent partitioning of this pair into the stationary phase. Let us emphasize at the outset that our presentation of this simulation does not mean that we endorse an ion-pair mechanism of sample retention. Rather, we tend to agree with the proponents of the ion-interaction model in that the mechanism of retention is in reality dependent on a wide variety of experimental parameters and that for most practical separations retention of ionic solutes results from more than one process. The ion-interaction model of retention does not require that any particular mechanism be operative but accommodates all previously proposed mechanisms. The ion-pair model is chosen for this simulation mainly because of the ease of programming, and, since from thermodynamics equivalent results are predicted for all mechanisms, the ion-pair model was chosen as the most efficient means of implementing the calculations. The ion-pair model also has the advantage of being chemically intuitive.

The results of the simulation described below show that, from a thermodynamic perspective, the mechanistic details of the process are irrelevant. All of the effects observed by Stranahan and Deming[21] are inherent in the perturbation process, and it does not matter that the perturbation originates in the stationary phase or in the mobile phase.

The chief objectives of this study were: First to incorporate a buffer species into the model in order to see whether this could explain the existence of more than one system peak as observed in our experimental work. Second, and more importantly, to account for the gross variations in the analytical sensitivity of the visualization technique, as observed by Denkert *et al.*[8], Hackzell *et al.*[10], Bidlingmeyer and Warren[17,18] and by ourselves[13–16].

The derivation below assumes constant distribution coefficients for all species. Experimentally, we know that stationary phase saturation effects can occur[14–16]. This does not seem to affect the major qualitative features of the results. One added aspect of the ion-pair model simulation presented below is the inclusion of buffer ions in the mobile phase and their effect on the response and retention of the samples. Buffer ions were not accounted for in previous work[21] and can have a significant effect on sample retention as discussed in earlier reports[10,14–16,18].

The simulation described below is also based on a Craig-type repetitive distribution. It differs from that of Stranahan and Deming[21] in that a single two-dimensional array is used to represent the mobile and stationary phases of up to 100 "tubes" (array elements). This is a difference in execution only and has no bearing on the end result. The actual number of tubes or transfers can be specified. The "column" is equilibrated with the mobile phase so that the initial eluent concentration of each species is the same as that which will be introduced into the first mobile phase element of the array after each discrete transfer. To "inject" a sample, the analytical concentration of sample A is introduced into the first tube and the entire tube (both stationary and mobile phase elements of the array) is equilibrated. The mobile phase of the first tube is then transferred to the second tube and fresh eluent (containing no A) is added to the first tube. Tubes 1 and 2 are then equilibrated, and the transfer process is repeated with the equilibrated eluent from the second tube transferred to the third tube and that from the first to the second, etc. After transfer has been completed for all array elements, the total number of moles of IIR (X) in each tube is displayed graphically on a video monitor so that the progress of the vacancy and excess peaks can be monitored. After the specified number of transfers has been completed, the distribution of X as a function of tube number is again displayed (the result of the last transfer) and is then graphically presented on the Epson MX-80 dot matrix printer. In addition, data for the excess or deficiency of each species in each tube are printed, normalized to the amount of injected A. k' Values for sample A, buffer B and IIR (X) are also reported. The calculations and derivation for the ion-pair model are given below.

The basic equilibria for ion-pair formation in the mobile phase and subsequent partitioning of the pair into the stationary phase are as follows:

$$A + X \rightleftharpoons AX \quad [AX] = K_A[A][X] \tag{1}$$

$$AX \rightleftharpoons AX' \quad [AX'] = K_{AX}[AX] \tag{2}$$

$$B + X \rightleftharpoons BX \quad [BX] = K_B[B][X] \tag{3}$$

$$BX \rightleftharpoons BX' \quad [BX'] = K_{BX}[BX] \tag{4}$$

where A, B and X represent the mobile phase concentrations of the eluite ion, buffer ion, and IIR, respectively. Similarly, AX, BX, AX′ and BX′ represent the sample–IIR ion pair and buffer–IIR ion pair in the mobile and stationary phases, respectively. The formation constants for the eluite ion pair (K_A) and for the buffer ion pair (K_B),

as well as the partition equilibrium constants (K_{AX}, K_{BX}), are defined implicitly by eqns. 1–4. The mass balance equations are

$$N_A = V_S[AX'] + V_M([A] + [AX]) \quad (5)$$
$$N_B = V_S[BX'] + V_M([B] + [BX]) \quad (6)$$
$$N_X = V_S([AX'] + [BX']) + V_M([AX] + [BX] + [X]) \quad (7)$$

where V_M and V_S represent the volumes of mobile and stationary phase, respectively. N_A, N_B and N_X represent the total moles of A, B and X, respectively, in all forms. These seven equations provide a mathematically exact solution.

The concentrations of all species are obtained by an iterative method. Usually, only 2–3 iterations are needed, but ten are actually performed in the computer program for this simulation.

The initial, equilibrated column conditions before injection of A are obtained from the analytical concentrations of B and X, which make up the eluent that is constantly pumped through the column. The actual, steady-state eluent concentrations of each individual species ([B], [BX], [X]) are obtained by setting $N_A = 0$, assuming no partitioning of any species and using these values and the analytical concentrations of B and X in the same algorithm. The required steady-state stationary phase concentration of each species is then calculated from the steady-state eluent concentration and the partition coefficient of each species. The sample, A, is then introduced into the first tube and equilibrations and transfers are performed as described above.

Simulations were performed that investigated the retention of the sample as a function of ion-pair formation and partition equilibrium constants, concentration of buffer, and concentration of IIR. The sensitivity in terms of the area of the sample peak, normalized to the amount of injected sample as a function of k' relative to the k' of the IIR, was also determined. The results of these simulations were mentioned above but are discussed more fully below.

Fig. 4 contains representative plots of the IIR concentration as a function of tube number after 25 transfers for the cases where the sample-IIR pair is less retained (curve A), has the same retention (curve B), and is more retained (curve C) than the IIR-buffer ion pair. Our results, based on an ion-pair model, are qualitatively the same as the results of Stranahan and Deming for their general and ion-interaction model of retention. These three cases are detailed further below:

Case A, k' (eluite) < k' (IIR): the eluite peak is negative and the system peak is positive.

Case B, k' (eluite) = k'(IIR): the leading edge of the eluite emerges together with a negative (vacancy) peak, and the trailing edge of the eluite emerges together with the positive peak. The net response in this case is larger than either case A or C.

Case C, k' (eluite) > k' (IIR): the eluite peak is positive and the system peak is negative.

However, there is one major difference between our results and those obtained by Stranahan and Deming[21]. Our model, with the inclusion of buffer ions in the system, assumes that the IIR cannot be retained without either a buffer ion or eluite ion as a co-ion. Furthermore, it predicts, in accord with our experimental observa-

tions, that in addition to the eluite and IIR peaks a third peak at the void volume will also be observed upon injection of a sample. This void volume peak is always negative. Its origin is linked to the same phenomena that induces the eluite and IIR (system) peak. The void volume peak is in actuality a second system peak.

Upon injection of a sample into a column that is at steady-state, the presence of the sample will cause additional IIR to be transferred into the stationary phase. This effectively leaves a deficiency of IIR in the eluent. The buffer–IIR pair distribution must then reestablish equilibrium, and it does this by releasing some of the adsorbed buffer–IIR into the eluent, but not enough to reestablish the initial equilibrium concentration of IIR. Effectively, two system peaks are thus induced. Since there is a net deficiency of IIR in the eluent after the first tube has reestablished equilibrium with all species, and since neither the IIR nor the buffer ion can be retained unless it first forms an ion pair with the other, the local deficiency of IIR proceeds along the column unretained and emerges as the vacancy peak at the void volume of the column. The second system peak, which is retained, is due to the retention of the buffer–IIR pair and can be either positive or negative, depending on whether the sample ion or the buffer ion is more retained than the other.

The appearance of the void volume peak agrees very well with the experimental results presented in Fig. 2. In addition, the relative sensitivities of the eluite peak depending on its k' relative to that of the system peak also agree well with the experimental results. Specifically the sensitivity of the eluite peak in the experimental results is always smaller if the eluite emerges before the system peak than when it emerges after the system peak. This phenomena is easily understood for this simplified model of retention, because mass, and consequently area, of the peaks must be conserved. The sum of the areas for all the negative peaks must equal the sum of the areas of all the positive peaks.

In our model, where only one sample is injected at a time, if the sample is less retained than the system peak then the sample area is only part of the total negative area, but if the sample emerges after the system peak, the sample peak contains all of the positive area. The point at which the sample and system peaks have the same retention is clearly a critical point in terms of sample sensitivity, and the sample sensitivity *versus* k' is clearly a rapidly changing function in the region including the system peak k'.

The response factor curve in Fig. 4 is extremely interesting, because it predicts very well the curve obtained for a real system[8,10]. The sensitivity or response factor for a sample increases with k' goes through a maximum and then levels out to a constant value. The maximum should correspond to the point where the k' values of the sample and system peak are equal. The maximum in the curve in Fig. 4 occurs at a slightly lower k' than this point. This is due to the relatively small number of tubes used for the simulation (99 tubes), compared to the number of theoretical plates in a column. It was found that the maximum of this curve does shift towards the point of equal k' values and that the maximum becomes more packed with an increasing number of tubes or transfers. Fig. 4 shows this effect. This agrees well with the data obtained with real systems and with the simulation results of Stranahan and Deming[21] for the point of equal k' values.

The general effect of a decrease in sample k' with an increase in buffer concentration (Fig. 4) does agree with our own experimental results (see Fig. 2), but the

effect observed is more pronounced in a real system, as shown in previous reports[14–16], than in the results of this simulation.

In summary, the results of this ion-pair model simulation agree very well qualitatively with the results of Stranahan and Deming[21]. The only differences in our results are due to the inclusion of an excess of buffer in our model, which more closely approximates a real system. In terms of the final result of a simulation, the actual mechanistic model chosen to describe all the equilibria involved in the retention of a sample and the induction of the indicator peaks is shown to be irrelevant. The actual pathway or mechanism of retention does not matter in a thermodynamic sense since the thermodynamics of a system are unaffected by the way a system reaches equilibrium as long as it does. The model of retention that has been simulated in this work may not reflect reality, but the final result does.

Furthermore, the results of this simulation generally agree qualitatively with the experimental sensitivity results presented earlier in this report. The differences that do exist can be attributed to either the assumption that there are no stationary phase saturation effects, which is known to be false for certain cases in a real system[14–16], or to the low number of transfers in the simulation compared with the number of plates in a real column.

Response factors for sample ions are very strongly dependent on their k' relative to the system peaks. However, nearly constant response factors are obtained for eluites that emerge after the system peak.

An ideal chromatographic system for optimized detection and precision in UV-visualization chromatography would employ as low an eluent concentration of IIR as possible in order to maximize the extinction coefficient and, in turn, maximize the sensitivity for the samples. In addition, all samples should emerge after the system peak and, therefore, the system peak should emerge as early in the chromatogram as possible (preferrably with a $k' \leqslant 2$).

Chromatographic simulations were performed that predict quite accurately the types of induced peaks and response factors for the peaks resulting from the separation and detection of inorganic anions by UV-visualization chromatography.

ACKNOWLEDGEMENTS

This work was supported by a grant from the National Institute of Occupational Safety and Health (RO1-OH-00876-OH), a grant from the 3M Company and summer support for W.E.B., provided by the Dow Chemical Company.

REFERENCES

1 R. N. Reeve, *J. Chromatogr.*, 177 (1979) 393.
2 N. E. Skelly, *Anal. Chem.*, 54 (1982) 712.
3 H. J. Cortez, *J. Chromatogr.*, 234 (1982) 517.
4 Z. Iskandarani and D. J. Pietrzyk, *Anal. Chem.*, 54 (1982) 2427.
5 R. A. Cochrane and D. E. Williams, *J. Chromatogr.*, 241 (1982) 392.
6 H. Small and T. E. Miller, Jr., *Anal. Chem.*, 54 (1982) 462.
7 N. Parris, *Anal. Biochem.*, 100 (1979) 260.
8 M. Denkert, L. Hackzell, G. Schill and E. Sjögren, *J. Chromatogr.*, 218 (1981) 31.
9 B. Sachok, S. N. Deming and B. A. Bidlingmeyer, *J. Liq. Chromatogr.*, 5 (1982) 389.
10 L. Hackzell, T. Rydberg and G. Schill, *J. Chromatogr.*, 282 (1983) 179.

11 L. Hackzell and G. Schill, *Chromatographia*, 15 (1982) 437.
12 N. Parris, *J. Liq. Chromatogr.*, 3 (1980) 1743.
13 W. E. Barber and P. W. Carr, *J. Chromatogr.*, 260 (1983) 89.
14 W. E. Barber and P. W. Carr, *Paper No. 69, Eastern Analytical Symposium, New York City, November 1983.*
15 W. E. Barber, *Ph.D. Thesis*, University of Minnesota, Minneapolis, MN, 1983.
16 W. E. Barber and P. W. Carr, *J. Chromatogr.*, 301 (1984) 25.
17 B. A. Bidlingmeyer and F. V. Warren, Jr., *Anal. Chem.*, 54 (1982) 2351.
18 F. V. Warren, Jr. and B. A. Bidlingmeyer, *Anal. Chem.*, 56 (1984) 487.
19 M. Dreux, M. LaFosse and M. Pequignot, *Chromatographia*, 15 (1982) 653.
20 C. N. Reilley, G. P. Hildebrand and J. W. Ashley, *Anal. Chem.*, 34 (1962) 1198.
21 J. J. Stranahan and S. N. Deming, *Anal. Chem.*, 54 (1982) 1541.
22 A. Hubaux and G. Vox, *Anal. Chem.*, 42 (1970) 849.
23 L. D. Rothman, S. R. Crouch and J. D. Ingle, Jr., *Anal. Chem.*, 47 (1975) 1226.
24 B. A. Bidlingmeyer, S. N. Deming, W. P. Prize, Jr., B. Sachok and M. Petrusek, *J. Chromatogr.*, 186 (1979) 419.
25 B. A. Bidlingmeyer, *J. Chromatogr. Sci.*, 18 (1980) 525.
26 J. J. Stranahan and S. N. Deming, *Anal. Chem.*, 54 (1982) 2251.